Tritylpyridinium tetrakis(pentafluorophenyl)borate as an efficient activator for "constrained-geometry" catalysts in ethylene polymerization

Kittichote Musikabhumma, Thomas P. Spaniol, Jun Okuda*

Institut für Anorganische Chemie und Analytische Chemie, Johannes Gutenberg-Universität Mainz, Duesbergweg 10-14, Mainz D-55099, Germany

Abstract

Ethylene polymerization with linked amido-cyclopentadienyl or "constrained-geometry" titanium catalysts, $Ti(\eta^5:\eta^1-C_5Me_4SiMe_2N^tBu)X_2$ (X = Me, Bz, Cl), activated by tritylpyridinium tetrakis(entafluorophenyl)borate, $[Ph_3C(NC_5H_5)] [B(C_6F_5)_4]$, and silica-supported tritylpyridinium tetrakis(entafluorophenyl)borate (PySTB) was found to proceed with high activity. ^1H NMR spectra in CD_2Cl_2 suggest that $([Ti(\eta^5:\eta^1-C_5Me_4,SiMe_2N^tBu)Me (NC_5H_5)]^+$ is formed as the main cationic species. Using the heterogeneous cocatalyst PySTB in hexane, unexpectedly high ethylene polymerization activity was achieved, giving high molecular weight polyethylenes with excellent morphology and high bulk density (up to $0.46 g/cm^3$).

© 2003 Elsevier B.V. All rights reserved.

Keywords: Borate activators; Catalysts; Ethylene polymerization; Polyethylene; Supported catalyst

1. Introduction

Recently we have reported a comparative study on homogeneous and heterogeneous ethylene polymerization using linked amido-cyclopentadienyl or "constrained-geometry" titanium catalysts, $Ti(\eta^5:\eta^1-C_5Me_4SiMe_2NR)X_2$ (R = Me, ^iPr, ^tBu; X = Me, Bz, Cl) (for reveiws, see [1]), activated by trityl tetrakis pentafluorophenyl)borate, $[Ph_3C][B(C_6F_5)_4]$, and silica-supported borate, $\equiv Si–O–B(C_6F_5)_3^- Ph_3C^+$ (B-Sylopol). The strong methyl-abstracting trityl cations in $[Ph_3C][B(C_6F_5)_4]$ and $\equiv Si–O–B(C_6F_5)_3^- Ph_3C^+$ resulted in the efficient formation of the cationic alkyl titanium species [2]. There are several reports on the property of tritylpyridinium perchlorate and tetrafluoroborate, $[Ph_3C(NC_5H_5)]A$ (A = ClO_4, BF_4), as tritylating agents which have advantages over trityl chloride, Ph_3CCl [3–7]. We wondered whether the combination of the tritylpyridinium cation with the weakly coordinating counter-anion tetrakis(pentafluorophenyl)borate, $B(C_6F_5)_4$, used in metallocene-catalyzed olefin polymerization [8–10], would have

an effect on the polymerization activity of the titianium catalysts based on linked amido cyclopentadienyl ligand. Previously we had noted good ethylene polymerization activity when $Ti(\eta^5:\eta^1-C_5Me_4SiMe_2N^tBu)Me_2$ was activated in situ with $[Ph_3C][B(C_6F_5)_4]$ in the presence of pyridylethylsilane-modified silica [2b]. We report here the efficient ethylene polymerization with linked amido-cyclopentadienyl titanium catalysts activated by tritylpyridinium tetrakis(pentafluorophenyl)borate and by silica-supported tritylpyridinium tetrakis(pentafluorophenyl)borate (PySTB).

2. Experimental

2.1. General considerations

All manipulations were performed under argon atmosphere in a glovebox or by standard Schlenk techniques. Toluene and hexane were purified by distillation under argon atmosphere over sodium sand. Diethyl ether (Et_2O) was purified by distillation under argon atmosphere over sodium/benzophenone ketyl. Pyridine was distilled under argon from CaH_2 prior to use. Linked amido-cyclopentadienyl

---

* Corresponding author. Tel.: +49-6131-393-737;
fax: +49-6131-39-25605.

E-mail address: okuda@mail.uni-mainz.de (J. Okuda).

titanium dimethyl, dibenzyl, and dichloro complexes Ti(η^5:η^1-C$_5$Me$_4$SiMe$_2$N^{t}Bu)X$_2$ (X = Me, Bz, Cl) were synthesized according to established procedures [11–14]. Trityl tetrakis(pentafluorophenyl)borate, [Ph$_3$C] [B(C$_6$F$_5$)$_4$], triisobutylaluminum (TIBA), 4-{2-(trichlorosilyl)ethyl}-pyridine, Cl$_3$SiC$_2$H$_4$C$_5$H$_4$N, 25 wt.% in toluene, and chlorotrimethylsilane were purchased from commerical sources and used as received. Highly pure grade ethylene from Linde AG and other chemical reagents were used without any further purification. Sylopol$^®$ 948 silica, donated by GRACE GmbH (300 m^2/g surface area, 20 nm pore diameter, 50 μm particle size) was calcined under air atmosphere at 500 °C for 5 h and dried under vacuum at 200 °C for 6 h prior to use. The silanol content ($\equiv$Si–OH) of the calcined silica material was determined by thermo-gravimetric method [15] and estimated to be 1.18 mmol/g.

2.2. Tritylpyridinium tetrakis(pentafluorophenyl)borate [Ph$_3$C(NC$_5$H$_5$)][B(C$_6$F$_5$)$_4$]

The sample for ^{14}N NMR measurement was prepared by addition of slight excess of pyridine to a solution of [Ph$_3$C][B(C$_6$F$_5$)$_4$] (300 mg, 0.325 mmol) in 1–2 ml of toluene-d$_8$. Colorless crystals precipitated from the clear solution after 30 min. After standing overnight, the colorless crystals were isolated by filtration, washed with toluene and dried in vacuo to give [Ph$_3$C(NC$_5$H$_5$)][B(C$_6$F$_5$)$_4$]; yield 215 mg (66%). Anal. Calcd. for C$_{48}$H$_{20}$NF$_{20}$B: C, 57.57; H, 2.01; N, 1.40. Found: C, 57.06; H, 2.20; N, 1.51. ^{1}H NMR (CD$_2$Cl$_2$, −30 °C): δ 8.71 (d, $^3J_{HH}$ = 6.0 Hz, 2H, α-NC$_5$H$_5$$^+$), 8.53 (t, $^3J_{HH}$ = 8.0 Hz, 1H, γ-NC$_5$H$_5$$^+$), 7.98 (t, $^3J_{HH}$ = 7.2 Hz, 2H, β-NC$_5$H$_5$$^+$), 7.5–7.4 (m, 9H, *meta*- and *para*-Ph$_3$C), 7.11 (d, $^3J_{HH}$ = 7.2 Hz, 6H, *ortho*-Ph$_3$C). ^{1}H NMR (CD$_2$Cl$_2$, 25 °C): δ 8.72 (br, 2H, α-NC$_5$H$_5$$^+$), 8.53 (br, 1H, γ-NC$_5H_5$$^+$), 7.97 (br, 2H, β-NC$_5H_5$$^+$), 7.49 (br, 9H, *meta*- and *para*-Ph$_3$C), 7.12 (br, 6H, *ortho*-Ph$_3$C). ^{1}H NMR (CD$_2$Cl$_2$, 40 °C): δ 8.74 (br, 2H, α-NC$_5$H$_5$$^+$), 8.52 (br, 1H, γ-NC$_5H_5$$^+$), 7.99 (br, 2H, β-NC$_5H_5$$^+$), 7.49 (br, 9H, *meta*- and *para*-Ph$_3$C), 7.14 (br, 6H, *ortho*-Ph$_3$C). ^{13}C NMR (CD$_2$Cl$_2$, −30 °C): δ 149.16 (*ipso-C, Ph$_3$C*), 147.12 (γ-NC$_5$H$_5$$^+$), 144.68 (α-NC$_5H_5$$^+$), 138.06 (β-NC$_5H_5$$^+$), 137.51, 135.06 (C$_6F_5$), 130.17 (*ortho-Ph$_3$C*), 129.47 (*meta-Ph$_3$C*), 127.93 *para-Ph$_3$C*), 90.06 (Ph$_3$C). ^{19}F NMR (CD$_2Cl_2$, −30 °C): δ −133.77 (*ortho-C$_6$F$_5$*), −163.39 (t, $^3J_{FF}$ = 18.8 Hz, *para-C$_6$F$_5$*), −167.35 (d, $^3J_{FF}$ = 15.1 Hz, *meta-C$_6$F$_5$*), Δδ(*p-*, *m-*F) = 3.96. ^{19}F NMR (CD$_2$Cl$_2$, 25 °C): δ-133.47 (*ortho-C$_6$F$_5$*), −163.90 (t, $^3J_{FF}$ = 18.8 Hz, *para-C$_6$F$_5$*), −167.83 (t, $^3J_{FF}$ = 18.8 Hz, *meta-C$_6$F$_5$*), Δδ (*p-,m-*F) = 3.93. ^{14}N NMR (CD$_2$Cl$_2$, 25 °C): δ 228.

2.3. In situ generation of the cationic titanium species

To a cooled solution (−30 °C) of [Ph$_3$C (NC$_5$H$_5$)]-[B(C$_6$F$_5$)$_4$] (73 mg, 0.076 mmol) in 0.5 ml of CD$_2$Cl$_2$, was added a solution of Ti(η^5:η^1:C$_5$Me$_4$SiMe$_2$N^{t}Bu)Me$_2$ (23 mg, 0.069 mmol) in 0.3 ml of CD$_2$Cl$_2$ in the glovebox.

The mixture was then transferred into a tube, pre-cooled to −30 °C and the measurement carried out between −30 and 25 °C. ^{1}H NMR (CD$_2$Cl$_2$, 25 °C): δ 8.73 (br, 2H, α-NC$_5$H$_5$$^+$), 8.50 (br, 1H, γ-NC$_5H_5$$^+$), 8.22 (t, $^3J_{HH}$ = 8.0 Hz, 3H, *para*-Ph$_3$C$^+$), 8.04 (d, $^3J_{HH}$ = 4.8 Hz, 2H, α-TiNC$_5$H$_5$), 7.95 (br, 2H, β-NC$_5$H$_5$$^+$), 7.75 (t, $^3J_{HH}$ = 6.0 Hz, 6H, *meta*-Ph$_3$C$^+$), 7.65 (d, $^3J_{HH}$ = 8.4 Hz, 6H, *ortho*-Ph$_3$C$^+$), 7.48 (br, γ-TiNC$_5$H$_5$ and γ-NC$_5$H$_5$), 7.3-7.1 (m, Ph$_3$C and β-NC$_5$H$_5$), 2.46 (s, 3H, Ph$_3$C*Me*), 2.17, 2.13, 1.82, 1.53 (s, 4 × 3H, C$_5$Me$_4$), 1.45 (s, 9H, CMe$_3$), 1.18 (s, 3H, Ti*Me*), 0.82 (s, 2 × 3H, SiMe$_2$). ^{19}F NMR (CD$_2$Cl$_2$, 25 °C): δ-133.34 (*ortho*-C$_6$F$_5$), −164.07 (t, $^3J_{FF}$ = 18.8 Hz, *para*-C$_6$F$_5$), −167.93 (*meta*-C$_6$F$_5$), Δδ (*p-*,*m-*F) = 3.86.

2.4. Preparation of pyridylethylsilane-modified silica (PyS)

Pyridylethylsilane-modified silica (PyS) was prepared as previously described in ref. [2b]. The solid-state ^{29}Si NMR spectrum showed the signal of pyridylethylsilyl groups $\equiv$**Si**-C$_2$H$_4$-C$_5$H$_4$N) grafted on silica surface at −54 ppm and that of trimethylsilyl groups ($\equiv$**Si**(CH$_3$)$_3$), which were also introduced on the silica surface, at −15 ppm.

2.5. Preparation of silica-supported tritylpyridinium borate (PySTB)

To a toluene suspension of 0.9 g content (N content = 0.576 mmol) of pyridylethylsilane-modified silica, was added 40 ml toluene solution of [Ph$_3$C][B(C$_6$F$_5$)$_4$] (0.637 g, 0.691 mmol) via syringe at room temperature. The suspension was then heated to 60 °C, and stirred for 6 h. After cooling down to room temperature, the suspension was kept stirring for overnight. The change of the color from dark red to dark yellow-green was observed. After decantation, washing several times with toluene and drying in vacuo, the silica-supported tritylpyridinium borate (PySTB) could be obtained as pale yellow-green solid particles. The boron content was determined by HR-ICP -MS to be 0.16 mmol/g.

2.6. Ethylene polymerization procedures

Ethylene polymerization was carried out in a 100 ml Büchi glass reactor equipped with a magnetic stirrer. The catalyst preparation and aging steps were performed in the glovebox. For the homogeneous polymerization, the required amounts of solvent, TIBA, toluene stock solution of titanium complex and toluene solution of mixed [Ph$_3$C][B(C$_6$F$_5$)$_4$] and pyridine were added into the reactor following this order, and aged at 25 °C for 15 min. Then, the reactor was transferred out of the glovebox, and placed in the oil bath on the magnetic stirrer to perform the polymerization. In the case of heterogeneous polymerization, the required amounts of PySTB, solvent and toluene stock solution of titanium complex were, respectively, added, followed by aging of the catalyst at room temperature (25 °C) for 15 min. Then, TIBA

was added in the last order. Polymerization was started after introducing ethylene into the evacuated reactor, and the pressure was controlled by the pressure regulator and kept constant at 5 bar throughout the polymerization time. Termination was performed by venting the reactor and adding 1 ml of methanol. The polymerization mixture was transferred into a large amount of acidified methanol, and the precipitated polyethylene was filtered and washed several times with methanol, followed by drying at 70 °C in air to constant weight.

2.7. Analysis

^{1}H, ^{13}C; ^{19}F and NMR spectra were recorded on a Bruker DRX-400 spectrometer operating at 400.13, 100.62, 376.45 and 28.91 MHz, respectively. Chemical shifts for ^{1}H and ^{13}C NMR spectra were referenced using internal solvent resonances and are reported relative to tetramethylsilane. ^{19}F and ^{13}C NMR spectra were referenced to $CFCl_3$ and NH_3, respectively. NMR measurements of all air-sensitive samples were carried out in tubes with Teflon-sealed caps. CP-MAS solid-state ^{29}Si NMR spectra (79.4 MHz) were recorded on a Bruker ASX-400 spectrometer operating at a field of 9.4 T. High-resolution-inductively coupled plasma-mass spectrometry (HR-ICP-MS) was run on an Element 2 (Thermo Finnigan Bremen, Germany) by P. Klemens of this department. Infrared spectroscopy (IR) was run on a Mattson Galaxy 2030 FT-IR spectrometer. Elemental analysis was performed on a Heraeus Vario EL. Molecular weights (M_w) and molecular weight distributions (M_w/M_n) of the resulting polyethylenes were determined by high temperature GPC (PL-GPC210) at 135 °C using 1,2,4-trichlorobenzene as solvent by A. Jekel of the Center for Catalytic Olefin Polymerization at the Rijksuniversiteit Groningen, the
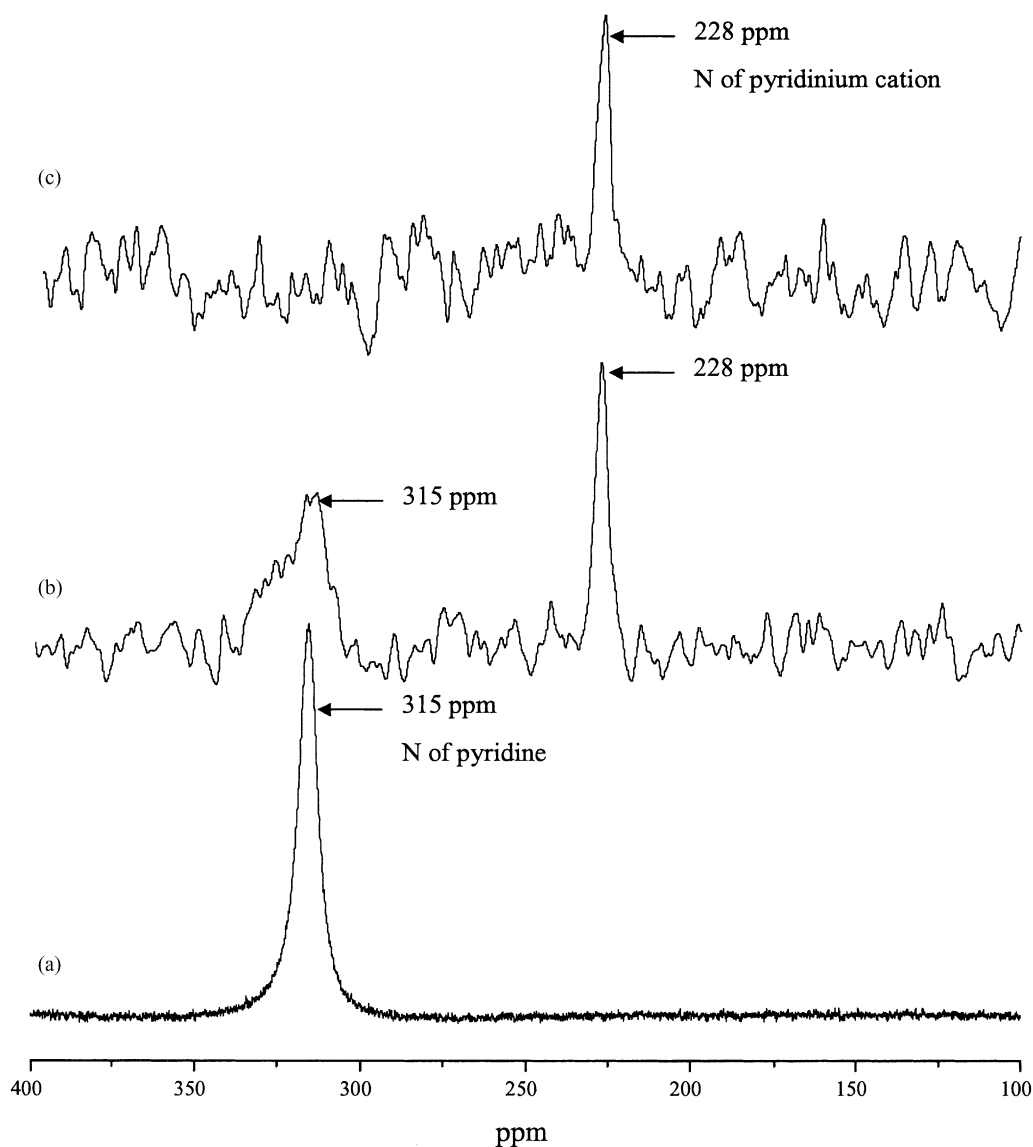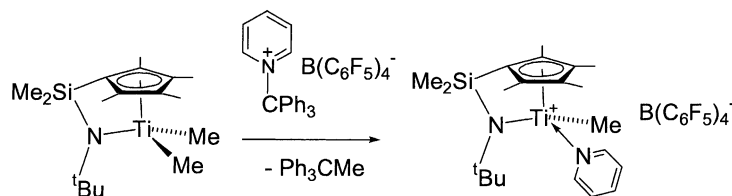

Fig. 1. ^{14}N NMR spectra of (a) free pyridine, (b) [Ph$_3$C(NC$_5$H$_5$)][B(C$_6$F$_5$)$_4$] formed in situ, (c) isolated [Ph$_3$C(NC$_5$H$_5$)][B(C$_6$F$_5$)$_4$] (in CD$_2$Cl$_2$ at 25 °C).
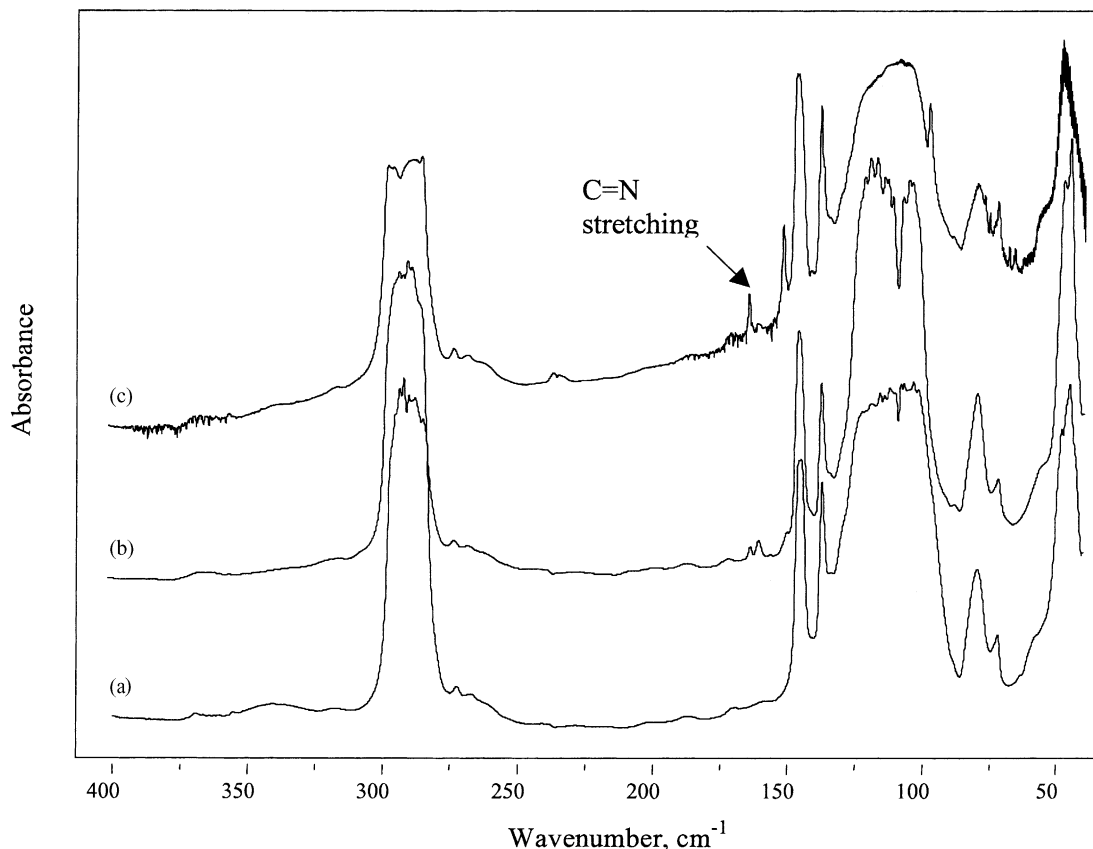
Scheme 1.

Fig. 2. IR spectra of (a) lithiated silica, (b) pyridylethylsilane-modified silica (PyS), (c) silica-supported tritylpyridinium borate (PySTB).

Netherlands. The crystalline melting temperature (T_m) and crystallinity (X_c) of the polymer were determined by differential scanning calorimetry (DSC, NETZSCH DSC204) under nitrogen at $10\,^\circ$C/min heating rate. The morphology of the polymer particles was examined on a LEO 1530 Gemini scanning electron microscope (SEM) by G. Glasser of the Max-Planck-Institut für Polymerforschung. The polymer bulk density was determined by weighing the polymer particles in the DSC aluminum pan of known volume.

3. Results and discussion

3.1. Generation of titanium alkyl cations by [Ph₃C(NC₅H₅)][B(C₆F₅)₄]

Addition of pyridine to a solution of the trityl tetrakis(pentafluorophenyl)borate [Ph₃C][B(C₆F₅)₄] afforded colorless

crystals of the composition [Ph₃C(NC₅H₅)][B(C₆F₅)₄]. The ¹⁴N NMR spectra of pyridine and tritylpyridinium salt [Ph₃C(NC₅H₅)][B(C₆F₅)₄] formed in situ in toluene-d₈ and isolated from the NMR sample are shown in Fig. 1.[1] The resonance of the nitrogen for free pyridine in CD₂Cl₂ solution was observed at 315 ppm (spectrum a). The spectrum b for [Ph₃C (NC₅H₅)] [B(C₆F₅)₄] shows that beside the resonance at 315 ppm due to the nitrogen of free pyridine, that of the nitrogen in the tritylpyridinium cation observed at higher field at 228 ppm. This resonance at 228 ppm was also observed in the spectrum c for the isolated [Ph₃C(NC₅H₅)][B(C₆F₅)₄]. By variable-temperature ¹H NMR spectroscopy (between -30 and $+40\,^\circ$C), [Ph₃C(NC₅H₅)][B(C₆F₅)₄] was found to be stable in CD₂Cl₂ solution. Neither the dissociation of

---

[1] Due to extremely low sensitivity of less abundant ¹⁵N isotope, highly concentrated NMR sarnple is required. Therefore, the ¹⁴N NMR spectroscopy was used in this study.

Table 1

Homogeneous ethylene polymerization with Ti(η^5:η^1-C$_5$Me$_4$SiMe$_2$N^{t}Bu)Me$_2$/[Ph$_3$C][B(C$_6$F$_5$)$_4$]/TIBA in the presence of pyridine[a]

Run number	Solvent	Py/B	Polymer time (min)	Yield (g)	Activity (kg PE/mol Ti h)	M_w ($\times 10^{-3}$)	M_w/M_n	T_m (°C)[b]	X_c (%)[c]
1	Toluene	0	30	0.495	198	156	3.1	138.4	61.7
2	Hexane	0	30	0.505	202	n.d.[d]	n.d.	137.8	78.1
3	Toluene	1	30	0.332	133[e]	n.d.	n.d.	136.0	83.1
4	Hexane	1	30	0.160	64	n.d.	n.d.	136.3	86.4
5	Toluene	0	7	0.260	446	279	4.9	138.1	69.9
6	Toluene	0.5	7	0.426	730	398	4.6	138.3	74.7
7	Toluene	1	7	0.329	564	209	4.0	137.3	70.4
8	Toluene	2	7	0.362	621	172	3.5	136.3	64.9

[a] Polymerization conditions: in 100 ml Büchi glass reactor, total volume 30 ml, ethylene pressure = 5 bar, polymer temperature = 70 °C, catalyst aging time (at 25 °C) = 15 min, Ti = 5 μmol, B/Ti = 2, Al/Ti = 200.
[b] Crystalline melting temperature.
[c] Crystallinity determined from X_c(%) = ($\Delta H_m/\Delta H_m^*$) × 100, ΔH_m^* = 293 J/g for HDPE.
[d] Not determined.
[e] The value is significantly lower than the real activity due to the formation of the gel-like product mixture after polymerization time of about 5 min.

tritylpyridinium cation to give free trityl cation and pyridine nor the formation of the ion–molecule pair was observed at 40 °C, suggesting a rapid equilibrium on the NMR time scale. The UV-Vis spectrum of the toluene solution of [Ph$_3$C(NC$_5$H$_5$)][B(C$_6$F$_5$)$_4$] prepared in situ showed the disappearance of the broad absorption band at λ_{max} = 430 nm attributed to the free trityl cation in solution, in agreement with the UV spectra of trityl perchlorate, [Ph$_3$C][ClO$_4$], and trityl tetrafluoroborate, [Ph$_3$C][BF$_4$], in CH$_2$Cl$_2$ [5].

The cationic titanium species [Ti(η^5:η^1-C$_5$Me$_4$SiMe$_2$N^t-Bu)Me(NC$_5$H$_5$)]$^+$[B(C$_6$F$_5$)$_4$]$^-$ was generated on the NMR scale by the reaction of Ti(η^5:η^1-C$_5$Me$_4$SiMe$_2$N^{t}Bu)Me$_2$ with [Ph$_3$C(NC$_5$H$_5$)][B(C$_6$F$_5$)$_4$] in CD$_2$Cl$_2$. At −30 °C, Ti(η^5:η^1-C$_5$Me$_4$SiMe$_2$N^{t}Bu)Me$_2$ did not react with [Ph$_3$C-(NC$_5$H$_5$)][B(C$_6$F$_5$)$_4$] in CD$_2$Cl$_2$ solution, as the peaks of α-, γ- and β-protons of the pyridinium cation were still observed at δ 8.70, 8.51 and 7.96 ppm. At room temperature, the formation of the cationic titanium species [Ti(η^5:η^1-C$_5$Me$_4$SiMe$_2$N^{t}Bu)Me(NC$_5$H$_5$)]$^+$ [B(C$_6$F$_5$)$_4$]$^-$ sets in. The singlet for the methyl protons of Ph$_3$CMe was observed at δ 2.46 ppm, confirming the methyl abstraction by the tritylpyridinium cation. The formation of a pyridine-coordinated cationic methyl titanium species

was confirmed by the singlet at 1.18 ppm. For the aromatic protons, the signals for the α-, γ- and β-protons of the pyridinium cation became small and broad, while the resonances of *ortho*-, *meta*- and *para*-phenyl protons of the free trityl cation became more intense [16,17]. These results indicate the generation of the cationic titanium species of [Ti(η^5:η^1-C$_5$Me$_4$SiMe$_2$N^{t}Bu)Me(NC$_5$H$_5$)]$^+$ (Scheme 1).

3.2. Preparation and characterization of silica-supported tritylpyridinium borate (PySTB)

The pyridylethylsilane-modified silica, obtained by modifying calcined silica with trichloropyridylethylsilane, was treated with [Ph$_3$C][B(C$_6$F$_5$)$_4$] in toluene. The silica-supported tritylpyridinium borate (PySTB) was obtained as pale yellow-green solid particles. The boron content of the PySTB was determined by HR-ICP-MS to be 0.16 mmol/g. As seen in the IR spectra in Fig. 2, the absorption band at about 1640 cm^{-1} due to the C=N stretching of pyridine ring of PySTB (spectrum c) was found to become remarkably sharper compared to that of the pyridylethylsilane-modified silica (spectrum b). This observation for the change of the C=N stretching absorption

Table 2

Homogeneous ethylene polymerization with Ti(η^5:η^1-C$_5$Me$_4$SiMe$_2$N^{t}Bu)X$_2$ (X Me, Bz, Cl)/[Ph$_3$C][B(C$_6$F$_5$)$_4$]/TIBA in the presence and absence of pyridine[a]

Run number	Ti catalyst	Py/B	Polymerization time (min)	Yield (g)	Activity (kg PE/mol Ti h)	M_w ($\times 10^{-3}$)	M_w/M_n	T_m (°C)[b]	X_c (%)[c]	Bulk density (g/cm^3)
1	X = Me	2	7	0.362	621	172	3.5	136.3	64.9	0.25
2	X = Bz	2	7	0.378	648	155	2.6	136.8	62.3	0.36
3	X = Cl	2	7	0.483	828	318	9.1[d]	135.4	81.1	0.26
4	X = Me	0	30	0.495	198	156	3.1	138.4	61.7	0.21
5	X = Bz	0	30	0.843	337	145	3.1	136.4	60.7	0.34
6	X = Cl	0	30	0.651	260	128	2.2	137.2	55.2	0.29

[a] Polymerization conditions: in 100 ml Büchi glass reactor, solvent toluene, total volume = 30 ml, ethylene pressure = 5 bar, polymerization temperature = 70 °C, catalyst aging time (at 25 °C) = 15 min, Ti = 5 μmol, B/Ti = 2, Al/Ti = 200.
[b] Crystalline melting temperature.
[c] Crystallinity determined from X_c(%) = ($\Delta H_m/\Delta H_m^*$) × 100, ΔH_m^* = 293 J/g for HDPE.
[d] Bimodal MWD.

band suggests the formation of positively charged pyridine nitrogen of the tritylpyridinium borate, $[Ph_3C(NC_5H_5)]$ $[B(C_6F_5)_4]$ [18].

3.3. Ethylene polymerization with $Ti(\eta^5:\eta^1-C_5Me_4SiMe_2N^tBu)Me_2$ activated by $[Ph_3C(NC_5H_5)][B(C_6F_5)_4]$

The results of ethylene polymerization with titanium dimethyl complex, $Ti(\eta^5:\eta^1-C_5Me_4SiMe_2N^tBu)Me_2$, activated by $[Ph_3C(NC_5H_5)][B(C_6F_5)_4]$, in the presence of TIBA as impurities scavenger are summarized in Table 1. As seen from the results in run 1 and 2, the polymerization without pyridine (Py/B = 0), i.e. with only $[Ph_3C][B(C_6F_5)_4]$ as activator, showed almost the same activities in toluene or hexane, whereas the polymerization at Py/B = 1 was found to be more efficient in toluene (run 3 and 4). The activity seemed to be higher than the result from run 1, but due to gel-formation after polymerization time of 5 min, the activity of run 3 appeared to be significantly lower. The effect of the ratio of pyridine to $[Ph_3C][B(C_6F_5)_4]$ (Py/B) on the polymerization activity and the properties of the resulting polyethylenes are shown in run 5–8. The activity increased from 446 kg PE/mol Ti·h to 730 kg PE/mol Ti·h upon the addition of pyridine to $[Ph_3C][B(C_6F_5)_4]$ at Py/B ratio of 0.5. The increase of Py/B ratio from 0.5 to 1 and 2 resulted in a drop of the activity to 564 and 621 kg PE/mol Ti·h, but still higher than the activity observed from run 5 (Py/B = 0). Varying the ratio of Py/B from 0 to 2 was also found to affect the molecular weights (M_w) and molecular weight distributions (MWDs, M_w/M_n) of the resulting polyethylenes. The M_w increased at Py/B = 0.5, but above this ratio it continuously decreased to the values lower than that of run 5 (Py/B = 0). The MWD was found to become narrower from 4.9 to 3.5 upon increasing the Py/B ratio
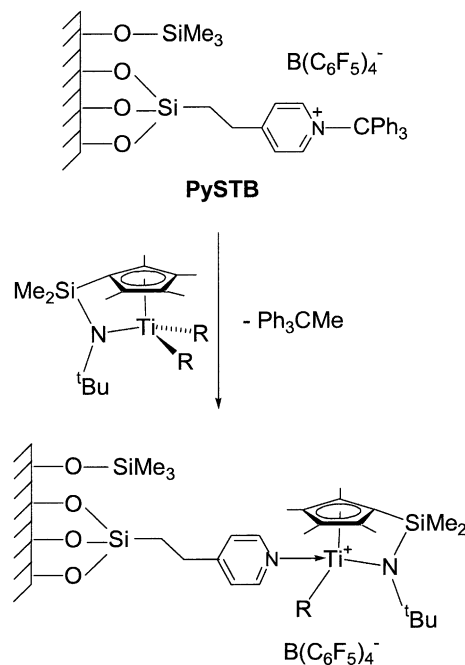
Scheme 2.

from 0 to 2. The melting temperatures (T_m) and cystallinities (X_c) of the resulting polyethylenes were found in the typical range of HDPE.

For comparison, the results of ethylene polymerization with titanium dimethyl, dibenzyl and dichloro complexes, $Ti(\eta^5:\eta^1-C_5Me_4SiMe_2N^tBu)X_2$ (X = Me, Bz, Cl), activated by $[Ph_3C(NC_5H_5)][B(C_6F_5)_4]$ and $[Ph_3C][B(C_6F_5)_4]$ [2] are summarized in Table 2. It is obvious that remarkably higher activities could be obtained in the presence of pyridine. The dichloro complex was found to give the highest activity of 828 kg PE/mol Ti·h (run 3), and the activity trend follows X = Cl > Bz > Me. In contrast, the

Table 3
Heterogeneous ethylene polymerization with $Ti(\eta^5:\eta^1-C_5Me_4SiMe_2N^tBu)X_2$ (X = Me, Bz, Cl)/PySTB/TIBA[a]

Run number	Ti catalyst	Solvent	Polymerization time (min)	Yield (g)	Activity (kg PE/mol Ti h)	M_w ($\times 10^{-3}$)	M_w/M_n	T_m (°C)[b]	X_c (%)[c]	Bulk density (g/cm^3)
1	X = Me	Toluene	30	0.090	36	458	6.4[d]	128.0[e]	30.3	0.27
2	X = Me	Hexane	30	2.765	1106	609	2.8	135.9	60.6	0.44
3	X = Bz	Toluene	30	0.124	50	896	5.7[d]	133.6	41.3	0.31
4	X = Bz	Hexane	30	3.105	1242	793	3.8	133.7	56.5	0.46
5	X = Cl	Toluene	30	0.070	28	529	6.6[d]	128.5[e]	30.4	0.22
6	X = Cl	Hexane	30	4.413	1765	429	3.2	137.8	69.2	0.39
7[f]	X = Me	Toluene	30	0.627	251	932	2.3	134.8	45.3	0.29
8[f]	X = Bz	Toluene	30	1.501	600	738	2.2	133.9	51.5	0.38
9[f]	X = Cl	Toluene	30	0.213	85	647	3.3	133.9	42.9	0.24

[a] Polymerization conditions: in 100 ml Büchi glass reactor, total volume = 30 ml, ethylene pressure = 5 bar, polymerization temperature = 70 °C, catalyst aging time (at 25 °C) = 15 min, Ti = 5 μmol, B/Ti = 2 (PySTB = 61 mg), Al/Ti = 200.
[b] Crystalline melting temperature.
[c] Crystallinity determined from $X_c(\%) = (\Delta H_m / \Delta H_m^*) \times 100$, $\Delta H_m^* = 293$ J/g for HDPE.
[d] Bimodal MWD.
[e] Shoulder at higher melting temperature was observed.
[f] Results obtained from B-Sylopol system under the same polymerization conditions [2].

dibenzyl complex was found to give the highest acitivity with $[Ph_3C]$ $[B(C_6F_5)_4]$ as activator, and the activity trend follows $X = Bz > Cl > Me$. Regarding the properties of the polyethylenes obtained from these two systems, the M_w, MWD, T_m, X_c and bulk density are observed almost in the same range. The dichloro complex in the presence of pyridine was found to give polyethylene with unusually broad and bimodal MWD (run 3). The above results indicate that the tritylpyridinium borate, $[Ph_3C(NC_5H_5)]$ $[B(C_6F_5)_4]$, is a more efficient activator than the trityl borate, $[Ph_3C][B(C_6F_5)_4]$, for the homogeneous ethylene polymerization with titanium catalysts. The higher activities observed might be due to stabilization of the titanium alkyl cations by coordinated pyridine, leading to longer life time of the active cationic species.

3.4. Ethylene polymerization with $Ti(\eta^5{:}\eta^1{-}C_5Me_4SiMe_2N^tBu)X_2$ ($X = Me, Bz, Cl$) activated by PySTB

The activation process by PySTB to form the silica-supported cationic titanium catalysts is shown in Scheme 2. The results of heterogeneous ethylene polymerization with titanium dimethyl, dibenzyl and dichloro complexes, $Ti(\eta^5{:}\eta^1{-}C_5Me_4SiMe_2N^tBu)X_2$ ($X = Me, Bz, Cl$), activated by PySTB in the presence of TIBA are summarized in Table 3. Polymerization in toluene was not efficient, as very low actitivities were observed for all three complexes. Polymerization in hexane resulted in high activities above 1000 kg PE/mol Ti·h for all three titanium complexes. The dichloro complex was found to give the highest activity of 1765 kg PE/mol Ti·h, which is about double of that
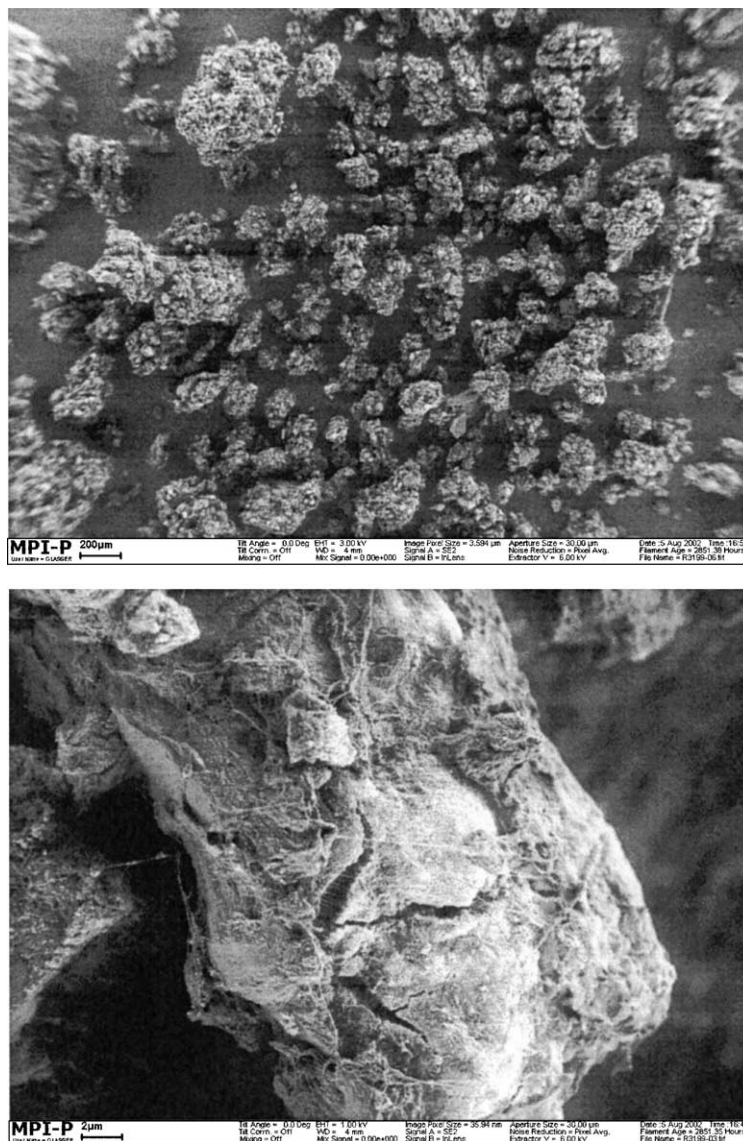

Fig. 3. SEM images of polyethylene obtained with $Ti(\eta^5{:}\eta^1{-}C_5Me_4SiMe_2N^tBu)Bz_2$/-PySTB/TIBA in toluene (run 3 in Table 3).

observed in the corresponding homogeneous system (run 3 in Table 2). The trend in activity for the polymerization in hexane was observed similar to that of the homogeneous system, i.e. X = Cl > Bz > Me. For the properties of the resulting polyethylenes, the molecular weights (M_w) of the resulting polyethylenes both obtained in toluene and hexane were found higher than those of the polyethylenes from homogeneous system, in the range of 4×10^5 to 9×10^5. Interestingly, the MWDs of the polyethylenes obtained in toluene were very broad in the range of 5–7 and observed as bimodal MWD curves. Those of the polyethylenes obtained in hexane were narrow in the typical range for single-site catalysts. The low activities together with broad and bimodal MWDs of polyethylenes obtained in toluene might be explained by the leaching of the cationic active titanium species from the silica surface. Toluene competes with the weakly coordinating pyridine on silica surface for the cationic titanium species. Such a leaching phenomenon,

which can be controlled by the basicity of the functionalized amine groups on the solid supports and the polarity of the polymerization medium, has recently been reported for ethylene polymerization with cationic hafnocenes supported on amine-functionalized polystyrene beads [19,20]. The melting temperatures (T_m) and crystallinities (X_c) of the polyethylenes obtained in toluene are rather low, whereas those of the polyethylenes obtained in hexane are typical for HDPE.

With respect to the morphology, the resulting polyethylenes obtained in hexane were found to exhibit good flowability and high bulk densities (>0.39 g/cm^3). The bulk density as high as 0.46 g/cm^3 could be achieved by the dibenzyl titanium catalyst (run 4). The SEM images of the resulting polyethylene obtained from run 3 in toluene (Fig. 3), shows some fine particles and a soft polyethylene layer, produced in the homogeneous phase due to the leaching, on the surface of the polymer particles. The SEM images
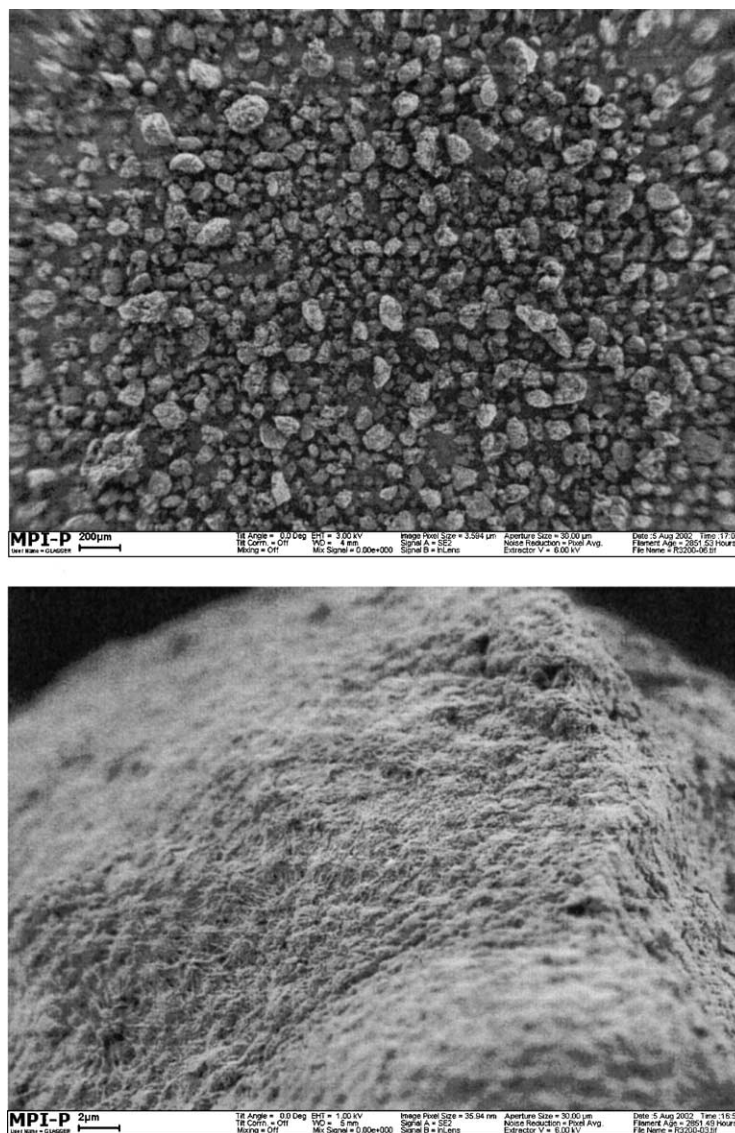

Fig. 4. SEM images of polyethylene obtained with Ti(η^5:η^1-C$_5$Me$_4$SiMe$_2$N^{t}Bu)Bz$_2$/PySTB/TIBA in hexane (run 4 in Table 3).

of the polyethylene obtained from run 4 in hexane (Fig. 4) shows improved morphology and more rigid surface of the polymer particles.

4. Conclusions

The ethylene polymerization activity with linked amido-cyclopentadienyl or "constrained-geometry" titanium catalysts significantly increased in the presence of [Ph$_3$C (NC$_5$H$_5$)][B(C$_6$F$_5$)$_4$]. The silica-supported tritylpyridinium borate (PySTB) was found to exhibit higher activity for ethylene polymerization in hexane when combined with the corresponding titanium catalysts than the previously reported B-Sylopol system [2]. This catalyst produced polyethylenes with excellent morphology and significantly higher bulk densities. The leaching of the cationic titanium catalyst was observed in toluene, leading to low activity and broad and bimodal MWD of the resulting polyethylene.

Acknowledgements

References

[1] (a) A.L. McKnight, R.M. Waymouth, Chem. Rev. 98 (1998) 2587;
(b) J. Okuda, T. Eberle, Metallocenes, in: A. Togni, R.L. Halterman (Eds.), Wiley, New York, 1998, p. 415.

[2] (a) K. Musikabhumma, T.P. Spaniol, J. Okuda, Macromol. Chem. Phys. 203 (2002) 115;
(b) K. Musikabhumma, T.P. Spaniol, J. Okuda, J. Mol. Cat. 192 (2003) 223.

[3] A. Streitwieser Jr., Solvolytic Displacement Reactions, McGraw-Hill, New York, 1962, p. 82.

[4] C.G. Swain, Y. Okamoto, J. Am. Chem. Soc. 92 (1970) 3409.

[5] Y. Okamoto, Y. Shimakawa, J. Org. Chem. 35 (1970) 3752.

[6] A.R. Katritzky, G. Musumaira, Chem. Soc. Rev. 13 (1984) 47.

[7] (a) A.R. Katritzky, B. Brycki, J. Am. Chem. Soc. 108 (1986) 7295;
(b) A.R. Katritzky, C.H. Watson, Z. Dega-Szafran, J.R. Eyler, J. Am. Chem. Soc. 112 (1990) 2471.

[8] A.R. Siedle, W.M. Lamanna, R.A. Newmark, J. Stevens, D.E. Richardson, M. Ryan, Macromol. Symp. 66 (1993) 215.

[9] J.C.W. Chien, W.-M. Tsai, M.D. Rausch, J. Am. Chem. Soc. 113 (1991) 8570.

[10] R.F. Jordan, C.S. Bajgur, R. Willet, B. Scott, J. Am. Chem. Soc. 108 (1986) 7410.

[11] J. Okuda, T. Eberle, T.P. Spaniol, Chem. Ber. 130 (1997) 209.

[12] (a) T. Eberle, T.P. Spaniol, J. Okuda, Eur. J. Inorg. Chern. 1998, p. 237.;
(b) A.L. McKnight, M.A. Masood, R.M. Waymouth, D.A. Straus, Organometallics 16 (1997) 2879;
(c) T. Eberle, Doctoral Thesis, University of Mainz, Germany, 1998.

[13] P.-J. Sinnema, Doctoral Thesis, Rijksuniversiteit Groningen, The Netherlands, 1999.

[14] J. Okuda, K. Musikabhumma, P.-J. Sinnema, Isr. J. Chem. 42 (2003) 383.

[15] C. du Fresne von Hohenesche, Diploma Thesis, University of Mainz, Germany, 1999.

[16] M. Bochmann, S.J. Lancaster, J. Organomet. Chem. 434 (1992) C1.

[17] S.J. Lancaster, M. Bochmann, J. Organomet. Chem. 654 (2002) 221.

[18] T. Balakrishnan, V. Rajendran, J. Polym. Sci. Part A: Polym. Chem. 35 (1997) 727.

[19] S.B. Roscoe, J.M.J. Frechet, J.F. Walzer, A.J. Dias, Science 280 (1998) 270.

[20] R.M. Kasi, E.B. Coughlin, Organometallics 22 (2003) 1534.